Acta Pharm. **70** (2020) 303-324

Original research paper

https://doi.org/10.2478/acph-2020-0026

Synthesis, *in vitro* safety and antioxidant activity of new pyrrole hydrazones

DIANA TZANKOVA[1]
STANISLAVA VLADIMIROVA[2]
DENITSA ALUANI[3]
YORDAN YORDANOV[3]
LILY PEIKOVA[1]
MAYA GEORGIEVA[1,*]

[1] *Department of Pharmaceutical Chemistry, Faculty of Pharmacy Medical University Sofia 1000 Sofia, Bulgaria*

[2] *Department of Organic Synthesis and Fuels, University of Chemical Technology and Metallurgy 1756 Sofia, Bulgaria*

[3] *Department of Pharmacology Pharmacotherapy and Toxicology Faculty of Pharmacy Medical University Sofia 1000 Sofia, Bulgaria*

Accepted September 12, 2019
Published online November 4, 2019

Six new *N*-pyrrolylhydrazide hydrazones were synthesized under micro synthesis conditions, assuring about 59–93 % yield, low harmful emissions and reagent economy. The structures of the new compounds were elucidated by melting points, TLC characteristics, IR, ^{1}H and ^{13}C NMR spectral data followed by MS data. The purity of the obtained compounds was proven by the corresponding elemental analyses. "Lipinski's rule of five" parameters were applied for preliminary evaluation of the pharmacokinetic properties of the target molecules. The initial *in vitro* safety screening for cytotoxicity (on HepG2 cells) and hemocompatibility (hemolysis assay) showed good safety of the new compounds, where ethyl 5-(4-bromophenyl)-1-(1-(2-(4-hydroxy-3-methoxybenzylidene)-hydrazineyl)-1-oxo-3-phenylpropan-2-yl)-2-methyl-1*H*-pyrrole-3-carboxylate (**4d**) and ethyl 5-(4-bromophenyl)-1-(1-(2-(2-hydroxybenzylidene)hydrazineyl)-1-oxo-3-phenylpropan-2-yl)-2-methyl-1*H*-pyrrole-3-carboxylate (**4a**) were the least toxic. The antioxidant activity in terms of radical scavenging activity (DPPH test) and reducing ability (ABTS) was also evaluated. The antioxidant protective potential of the compounds was next determined in different *in vitro* cellular-based models, revealing compounds **4d** and **3** [ethyl 5-(4-bromophenyl)-1-(1-hydrazineyl-1-oxo-3-phenylpropan-2-yl)-2-methyl-1*H*-pyrrole-3-carboxylate] as the most promising compounds, with **4d** having better safety profile.

Keywords: pyrrole hydrazones, DPPH, ABTS, cytotoxicity, microsomes, oxidative stress

Pyrroles and their derivatives represent one of the most important groups of *N*-heterocyclic compounds because of their remarkable antibacterial, antiviral, anti-inflammatory, antitumor, and antioxidant activities (1). Recent studies of different benzoxazolyl, benzothiazolyl, benzimidazolyl-pyrroles with amide structure have been reported, displaying greater antioxidant and radical scavenging activity when compared with the standard drug, ascorbic acid (2).

* Correspondence, e-mail: mgeorgieva@pharmfac.mu-sofia.bg

Hydrazones represent a special group of compounds in the Schiff´s base family. They are usually synthesized *via* condensation of primary amines with active carbonyl groups; they represent active pharmacophores and fragments for the development of new drugs (3). Hydrazone derivatives possess a wide variety of biological activities such as anticancer (4–7), antioxidant (8, 9), antimycobacterial (10, 11), anti-inflammatory (12), antidepressant (13), antihypertensive (14), antimicrobial (15, 16) and anticonvulsant activity (17, 18).

Despite scientists' efforts to increase the number of compounds in chemolibraries to obtain better results on the search for hits, most of the compounds are often discarded in clinical phase II due to pharmacokinetic problems. Thus, the current research approach is focused on finding the key points in a compound's pharmacokinetic and pharmacodynamic properties that can be set as standards for drug design. These processes are, sometimes, referred to as drug-likeness or drug-like molecules recognition (19) and are used as a start-up point in drug design of pharmacologically active molecules.

Many aspects of drug-like properties can be quantified through physicochemical indices and these, in turn, can be calculated *in silico*. Criteria such as the Lipinski's rule of five (20) can be used to filter libraries and remove molecules with predicted poor drug-like properties that serve only to waste valuable drug development resources (21). Physicochemical features, like hydrophobicity, electronic distribution, hydrogen bonding characteristics, molecule size and flexibility, are often applied as pharmacophoric properties indicating the similarity of a newly synthesized molecule to the known drugs. This similarity is often called drug-likeness and is a good predictive tool for the preliminary evaluation of the behavior of a new molecule in a living organism in regard to bioavailability, transport properties, affinity to proteins, reactivity, toxicity, metabolic stability and many others (20).

Oxidative stress represents the impaired balance between reactive oxygen species (ROS) formation and the capacity to overcome ROS-induced danger in the body. It plays a significant role in the pathogenesis and pathophysiology of different diseases, including cardiovascular, neurodegenerative, oncological, inflammatory, *etc*. (22, 23). Thus, the role of antioxidants in the prevention and treatment of oxidative stress-related conditions is continuously increasing and many efforts have been targeted on the synthesis of new antioxidants with low cytotoxicity (24–26). Among them, different compounds containing a pyrrole moiety have been reported to possess antioxidant activity (27, 28).

Different hydrazones have also been reported to exert antioxidant properties by free-radical scavenging mechanisms (29). Most probably, an azomethine group in the structure of hydrazones contributes to their potent antioxidant activity (30).

Beside their favorable pharmacological effects, many new drug candidates fail to complete the drug development process due to different safety concerns. Therefore, the preliminary assessment of potential toxicity is an important step in early safety evaluation of newly developed compounds. It is substantially easier to utilize cell-based *in vitro* models to examine sub-cellular events, compared to higher levels of biological organization, *i.e*., whole organisms. Different *in vitro* models comprising subcellular fractions (*i.e*., liver microsomes), transformed cell lines (*i.e*., immortalized human hepatocytes cell HepG2 cells) or primary cells (*i.e*., isolated blood cells) provide additional information and are a useful tool in preliminary safety assessment (31).

In this study, we aimed to combine the two active principles of pyrrole moiety and hydrazine pharmacophore in a series of pyrrolylhydrazide-hydrazones (**3**, **4a-g**) with potential antioxidant activity. The pharmacokinetic behavior of the new structures was predicted through the calculation of molecular descriptors defined in the "Lipinski's rule of five" as an appropriate tool to distinguish drug-like from non-drug-like substances. In addition, *in vitro* toxicity evaluation on HepG2 cells and hemolysis study were carried out as a part of the initial safety screening for hemocompatibility and cytotoxicity of the newly synthesized hydrazones. The antioxidant activity was evaluated using ABTS and DPPH tests for radical scavengers' activity. Different *in vitro* cellular-based models of H_2O_2--induced oxidative damage and Fe^{2+}/ascorbic acid-induced lipid peroxidation were applied for evaluation of the antioxidant protective potential of the compounds.

EXPERIMENTAL

Materials and methods

The final hydrazones were synthesized in a micro-scale synthesis apparatus (Aldrich Micro-LabKit, USA) assuring low harmful emissions and reagent economy. The melting points were measured in a capillary digital melting point apparatus IA 9200 (Electrothermal, UK) and were not corrected. The synthesis progress was controlled by TLC on aluminium sheets Silicagel 60 F_{254} (Merck, Germany), using $CHCl_3$/ethanol (10:1) as a mobile phase.

The IR spectra within 400–4000 cm^{-1} range were recorded on a Nicolet iS10 FT-IR spectrometer using ATR technique with Smart iTR adapter (Thermo Fisher Scientific, USA). ^1H and ^{13}C NMR spectra were registered on Bruker Spectrospin WM600 spectrometer (Bruker, Switzerland) at 600 MHz, as δ (ppm) relative to TMS as internal standard, and the coupling constants (J) are expressed in hertz (Hz). All NH protons were D_2O exchangeable. The related mass spectra were obtained from a 6410 Agilent LCMS triple quadrupole mass spectrometer (LCMS) with an electrospray ionization (ESI) interface (Agilent Technologies, USA). Elemental analyses were performed on Euro EA 3000-Single analyser (EuroVector S.p.A, Italy). All chemical names were generated by using the structure-to-name algorithm of ChemBioDraw Ultra software, Version 12.0, CambridgeSoft, PerkinElmer Company, USA. All commercial chemicals and reagents used as starting materials in this study were research-grade chemicals, purchased from Merck. The molecular descriptors were determined using the free web-based server Molinspiration Cheminformatics (Molinspiration Cheminformatics, Bratislava University, Slovak Republic) (32, 33). Human hepatoma cells HepG2 were purchased from ATCC (Manassas, VA, USA). HepG2 cells were grown according to the standard protocol. The cells were cultured in DMEM cell medium (4500 mg L^{-1} glucose, without L-glutamine) with 10 % fetal bovine serum, 2 mmol L^{-1} L-glutamine, 1 % penicillin/1 % streptomycin 100× at 37 °C in an atmosphere of 5 % CO_2 in a humidified incubator.

Animals

Male Wister rats (200–220 g) were provided by National Breeding Centre, Sofia, Bulgaria). They were housed under standard conditions of temperature (20 ± 5 °C), fed with standard pellet diet and free access to water. The experimental procedures were approved by the Institutional Animal Care and Use Committee at the Medical University,

Sofia, Bulgaria. The principles stated in the European Convention for the Protection of Vertebrate Animals used for Experimental and other Scientific Purposes (ETS 123) and Principles of Laboratory Animal Care (NIH publication #85–23, revised in 1985) were followed strictly throughout the experiment.

Syntheses

*2-(5-(4-Bromophenyl)-3-(ethoxycarbonyl)-2-methyl-1*H*-pyrrol-1-yl)-3-phenyl-propanoic acid* (***1***). – It was synthesized applying the classical Paal-Knorr cyclization procedure, as already explained (34). In the current synthesis, L-phenylalanine was used as a primary amine and ethyl 2-acetyl-4-(4-bromophenyl)-4-oxobutanoate was used as a β-dicarbonyl compound. The intermediate dicarbonyl molecule was prepared by C-alkylation of commercially available 2-bromo-1-(4-bromophenyl)ethanone with ethyl 3-oxobutanoate and the final β-dicarbonyl compound was used in situ.

*Ethyl 5-(4-bromophenyl)-1-(1-ethoxy-1-oxo-3-phenylpropan-2-yl)-2-methyl-1*H*-pyrrole-3-carboxylate (**2**).* – $SOCl_2$ (0.04 mol) was added dropwise at 0 °C, under intensive stirring, to 50 mL dry ethanol, used as a solvent. Thereafter, 0.01 mol of compound **1** was added immediately and the mixture was refluxed for 2–3 h to complete the reaction (TLC control). The solvent was removed under reduced pressure and the resulting oil was dissolved in chloroform and washed successively with 5 % solution of Na_2CO_3 and water. The organic layer was dried over Na_2SO_4 and evaporated under reduced pressure (34). The obtained compound **2** was used in the next step without isolation and additional purification.

*Ethyl 5-(4-bromophenyl)-1-(1-hydrazinyl-1-oxo-3-phenylpropan-2-yl)-2-methyl-1*H*-pyrrole--3-carboxylate (**3**).* – The initial carbohydrazide (**3**) was prepared by selective hydrazinolysis

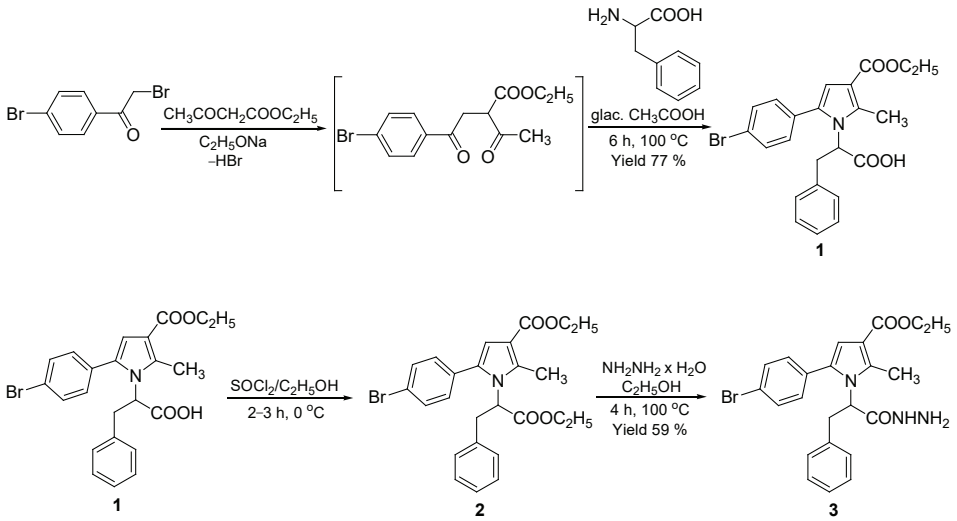

Scheme 1.

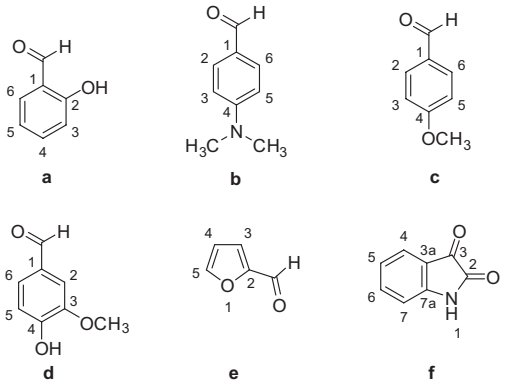

Fig. 1. Structures of the used carbonyl partners: 2-hydroxybenzaldehyde (**a**), 4-(dimethylamino)benzaldehyde (**b**), 4-methoxybenzaldehyde (**c**), 4-hydroxy-3-methoxybenzaldehyde (**d**), furan-2-carbaldehyde (**e**) and indoline-2,3-dione (**f**).

of the obtained ethyl ester **2**, according to the general procedure given in Scheme 1, as follows: 0.01 mol of the ethyl ester (**2**) and 0.02 mol hydrazine hydrate (100 %) were dissolved in 15 mL ethanol (99.7 %). The mixture was refluxed for 4 h to complete the hydrazinolysis of the remote ester group (TLC control). The product was isolated after cooling as a white solid and was recrystallized from ethanol.

*General procedure for the synthesis of the targeted hydrazones (**4a-f**).* – Equimolar quantities of carbohydrazide **3** and 1.8 mmol of either of the carbonyl partners 2-hydroxybenzaldehyde (**a**), 4-(dimethylamino)benzaldehyde (**b**), 4-methoxybenzaldehyde (**c**), 4-hydroxy-3-methoxybenzaldehyde (**d**), furan-2-carbaldehyde (**e**) or indoline-2,3-dione (**f**) (Fig. 1) were dissolved in 1.5 mL glacial acetic acid in a reaction vial of 5 mL and stirred at 100 °C for 40–50 min to complete the reaction (under TLC control) (Scheme 2). The products were isolated after adding water and recrystallized from ethanol.

Physico-chemical and spectral data are given in Tables I and II.

Drug-likeness estimation

The molecular descriptors and drug-likeness estimation of the target compounds were based on parameters calculated through Molinspiration Cheminformatics free based web server using the incorporated molecular processing and property calculation toolkits (32, 33).

Pharmacological evaluations

Cytotoxicity determination (MTT-dye reduction assay). – HepG2 cells were seeded in 96--well microplates at a density 2×10^4 cells per well, allowed to attach to the well surface for 24 h at 37 °C in a humidified atmosphere with 5 % CO_2. After incubation, different concentrations (1.0, 5.0, 10.0, 50.0, 75.0, 100.0, 250.0, 500.0 μmol L^{-1}) of the synthesized

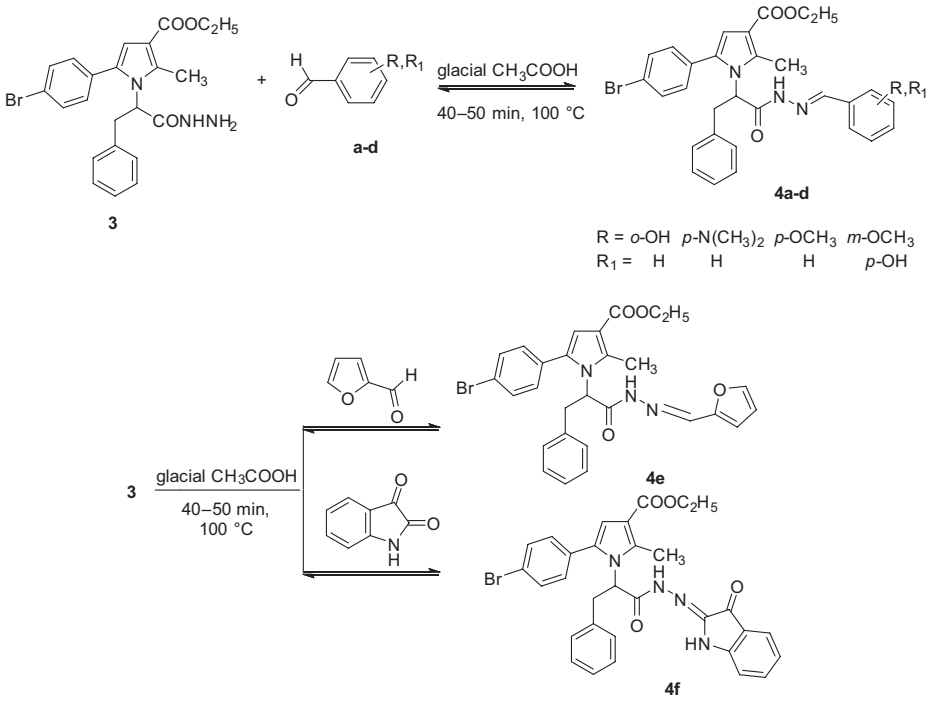

Scheme 2.

N-pyrrolylhydrazide hydrazones in DMSO were added to the cells and incubated for a period of 24 h (the final concentration of DMSO was below 0.5 %). At least 8 wells were used for each concentration. After the treatment, the culture medium was replaced by medium containing MTT solution and the cells were incubated for 3 h at 37 °C. Intracellularly formed formazan crystals were dissolved by the addition of 100 μL DMSO per well and absorbance was measured in a multiplate reader Synergy 2 (BioTek Instruments, USA) at 570 nm (690 nm for background absorbance).

In the oxidative stress model, cells (5×10^4 cells per well) were exposed to 0.1 mmol L^{-1} H_2O_2 for 1 h to obtain submaximal cytotoxicity (approximately 40 % *vs.* untreated controls). In order to estimate protection, cells were pre-treated for 1 h with the tested compounds **3**, **4a**-**f** (1–20 μmol L^{-1}) before the H_2O_2 pulse. Viability was assayed after 24 h by MTT-dye reduction assay. Data are normalized and are expressed as a percent of protection *vs.* H_2O_2 treatment (set as 0 %.)

Red blood cell hemolysis assay. – The hemolytic potential of the test substances was evaluated according to a protocol described by Evans *et al.* (35). Healthy volunteers' blood specimens were obtained from a certified clinical laboratory. The experimental procedures were approved by the Institutional Ethical Committee (KENIMUS) at the Medical University, Sofia, Bulgaria and conducted according to corresponding protocols. The erythrocytes were separated from whole blood by a series of centrifugations in 0.9 % NaCl

*Table I. Chemical names, melting points, yields and elemental analysis of new compounds **1**, **3** and **4a-f***

Code	Chemical name	Yield (%)	M. p. (°C)	Molecular formula (M_r)	C H N Br analysis calc./found (%)
1	2-(5-(4-Bromophenyl)-3-(ethoxycarbonyl)-2-methyl-1*H*-pyrrol-1-yl)-3-phenyl-propanoic acid	77	94.7–98.8	$C_{23}H_{22}BrNO_4$ 456.34	60.54 4.86 3.07 17.51 60.94 4.67 2.77 17.76
3	Ethyl 5-(4-bromophenyl)-1-(1-hydrazinyl-1-oxo-3-phenylpropan-2-yl)-2-methyl-1*H*-pyrrole-3-carboxylate	59	169.8–171.5	$C_{23}H_{24}BrN_3O_3$ 470.37	58.73 5.14 8.93 16.99 59.12 5.44 8.53 16.74
4a	(*E*)-ethyl 5-(4-bromophenyl)-1-(1-(2-(2-hydroxy benzylidene) hydrazinyl)-1-oxo-3-phenylpropan-2-yl)-2-methyl--1*H*-pyrrole-3-carboxylate	93	124.4–127.9	$C_{30}H_{28}BrN_3O_4$ 574.48	62.72 4.91 7.31 13.91 62.92 4.66 7.20 14.21
4b	(*E*)-ethyl 5-(4-bromophenyl)-1-(1-(2-(4-(dimethylamino) benzylidene) hydrazinyl)-1-oxo-3-phenylpropan-2-yl)--2-methyl-1*H*-pyrrole-3-carboxylate	68	184.9–187.2	$C_{32}H_{33}BrN_4O_3$ 601.54	63.89 5.53 9.31 13.28 63.75 5.77 9.20 13.68
4c	(*E*)-ethyl 5-(4-bromophenyl)-1-(1-(2-(4-methoxy benzylidene) hydrazinyl)-1-oxo-3-phenylpropan-2-yl)-2-methyl--1*H*-pyrrole-3-carboxylate	62	188.9–192.9	$C_{31}H_{30}BrN_3O_4$ 588.50	63.27 5.14 7.14 13.58 63.57 4.98 6.89 13.88
4d	(*E*)-ethyl 5-(4-bromophenyl)-1-(1-(2-(4-hydroxy-3-methoxy benzylidene) hydrazinyl)-1-oxo-3-phenylpropan-2-yl)-2-methyl-1*H*-pyrrole-3- carboxylate	74	124.0–127.9	$C_{31}H_{30}BrN_3O_5$ 604.50	61.59 5.00 6.95 13.22 61.81 4.80 6.70 13.52
4e	(*E*)-ethyl 5-(4-bromophenyl)-1-(1-(2-(furan-2-ylmethylene) hydrazinyl)-1-oxo-3-phenylpropan-2-yl)-2-methyl-1*H*-pyrrole-3-carboxylate	82	129.0–133.0	$C_{28}H_{26}BrN_3O_4$ 548.44	61.32 4.78 7.66 14.57 60.92 5.09 7.26 14.89
4f	(*E*)-ethyl 5-(4-bromophenyl)-2-methyl-1-(1-oxo-1-(2-(2-oxoindolin-3-ylidene) hydrazinyl)-3-phenylpropan-2-yl)-1*H*-pyrrole-3-carboxylate	85	243.7–247.2	$C_{31}H_{27}BrN_4O_4$ 599.49	62.11 4.54 9.35 13.33 62.30 4.89 9.25 13.12

Table II. Spectral data of new compounds 1, 3 and 4a-f

Compd.	IR (iATR) ν_{max} (cm^{-1})	^1H NMR $CDCl_3$, δ (ppm), J (Hz)	^{13}C NMR $CDCl_3$, δ (ppm), J (Hz)	MS (*m/z*)
1	3025, 2979, 1739, 1697, 818, 698	1.35 (t, 3H), 2.69 (s, 3H), 3.18–3.22 (m, 1H), 3.40 -3.43 (m, 1H), 4.25–4.33 (m, 2H), 4.93–4.95 (q, 1H, J = 4.11, J = 4.25), 6.36 (s, 1H), 6.55, 6.56 (d, 2H, J = 7.05), 6.67, 6.68 (d, 2H, J = 7.34), 7,13(t, 2H), 7.19 (t, 1H) 7.26 (s, 1H), 7.31,7.32 (d, 2H, J = 8.36)	174.6, 165.7, 135.9, 139.9, 134.0, 131.6, 131.3, 130.9, 128.9, 128.7, 127.1, 122.3, 109.8, 106.8, 59.8, 59.5, 36.8, 14.5, 13.2	458.08
3	3302, 3201, 2980, 1704 shoulder at 1680, 1570, 1238, 815, 697	1.35 (t, 3H), 2.65 (s, 3H), 3.13–3.17 (m, 1H), 3.61–3.64 (m, 1H), 3.76 (s, 2H), 4.26–4.31 (m, 2H), 4.77–4.80 (q, 1H, J = 3.67, J = 3.82), 6.40 (s, 1H), 6.42–6.45 (m, 2H), 6.71, 6.72 (d, 2H, J = 7.19), 7.14 (t, 2H), 7.20 (t, 1H), 7.26 (s, 1H), 7.29, 7.31 (d, 2H, J = 8.36)	170.3, 165.1, 136.5, 135.7, 134.3, 131.5, 131.3, 130.4, 129.1, 128.7, 127.1, 122.5, 114.7, 110.7, 60.3, 59.8, 36.1, 14.5, 13.5	472.10
4a	3434, 2975, 1683, 1661, 1573, 1246, 818, 750	1.34 (t, 3H), 2.66 (s, 3H), 3.12–3.17 (m, 1H), 3.68–3.73 (m, 1H), 4.23–4.27 (q, 2H, J = 7.04), 4.96–4.98 (q, 1H, J = 3.82, J = 3.96), 6.42 (s, 1H), 6.48 (s, 2H), 6.68, 6.69 (d, 2H, J = 7.34), 6.91 (t, 1H), 7.01–7.02 (d, 1H), 7.13 (t, 2H), 7.17–7.20 (m, 1H), 7.32–7.34 (m, 2H), 7.32–7.34 (m, 1H), 7.26 (s, 1H), 8.32 (s, 1H), 8.89 (s, 1H), 10.82–10.90 (m, 1H)	165.5, 165.2, 158.7, 152.3, 136.3, 136.0, 132.5, 131.7, 131.5, 131.4, 131.2, 131.1, 129.0, 128.7, 127.1, 122.6, 119.5, 118.3, 117.4, 116.9, 110.9, 60.7, 60.0, 36.2, 14.4, 13.4	576.13
4b	3290, 1709, 1674, 1569, 1250, 815, 698	1.35 (t, 3H), 2.08 (s, 6H), 2.71 (s, 3H), 3.13 (t, 1H), 3.53–3.55 (d, 1H, J = 11.3), 4.26–4.31 (m, 2H) 4.86–4.90 (q, 1H, J = 2.79, J = 3.23), 6.37 (s, 1H), 6.54 (s,2H), 6.64 - 6.65 (d, 2H, J = 7.34), 7.10–7.13 (m, 2H), 7.17–7.19 (m, 1H), 7.26 (s, 1H), 7.32–7.33 (d, 2H, J = 7.63), 7.81 (m, 1H), 8.18–8.20 (m, 2H), 8.22–8.29 (m, 2H)	167.9, 167.6, 165.2, 136.1, 136.0, 134.4, 131.5, 131.3, 130.3, 128.9, 128.9, 128.9, 128.7, 127.1, 122.5, 122.4, 114.8, 110.7, 77.5, 60.1, 59.9,36.1, 20.8, 14.5,13.6	601.18
4c	3280, 1717, 1668, 1570, 1250, 812, 700	1.34 (t, 3H), 2.07 (s, 3H), 2.70 (s, 3H), 3.12 (t, 1H), 3.52–3.55 (q, 1H, J = 2.65, J = 3.08), 4.25–4.31 (q, 2H, J = 6.89, J = 7.19) 4.87–4.90 (q, 1H, J = 3.23, J = 3.37), 6.37 (s, 1H) 6.54 (s, 2H), 6.63, 6.64 (d, 2H, J = 7.33), 6.74–6.77 (d, 1H, J = 19.08) 7.10–7.13 [(m, 2H), 7.16–7.19 (m, 1H), 7.26 (s, 1H), 7.31–7.33 (d, 2H, J = 7.78), 7.82–7.87 (m, 2H), 8.17–8.22 (d, 2H, J = 32.43)	167.9, 167.6, 165.2, 136.1, 136.0, 134.4, 131.5, 131.3, 130.3, 129.2, 128.9, 128.7, 128.7, 128.7, 127.1, 122.5, 114.8, 110.7, 95.7, 60.1, 59.9, 50.3, 36.0, 14.5, 13.6	588.15

Compd.	IR (iATR) ν_{max} (cm^{-1})	^1H NMR $CDCl_3$, δ (ppm), J (Hz)	^{13}C NMR $CDCl_3$, δ (ppm), J (Hz)	MS (*m*/*z*)
4d	3523,3192, 1694, 1660, 1568, 1241, 812, 697	1.32–1.36 (m, 3H), 2.70 (s, 3H), 2.76 (s, 1H), 3.16–3.21 (m, 1H), 3.42–3.45 (q, 1H, J = 4.4, J = 4.7), 3.94 (s, 3H), 4.25–4.30 (m, 2H), 4.93–4.95 (q, 1H, J = 3.08, J = 3.66), 6.38 (s, 1H), 6.45 (s, 2H), 6.68–6.71 (q, 2H, J = 7.19, J = 7.48) 7.11–7.15 (m, 2H), 7.19 (m, 1H), 7.26 (m, 1H), 7.27–7.28 (d, 2H, J = 8.51), 7.32, 7.34 (d, 2H, J = 8.07), 7.46 (s, 1H), 8.56 (m, 1H)	165.7, 165.6, 165.1, 147.1, 136.9, 136.5, 133.2, 131.6, 131.6, 131.5, 131.2, 129.1, 129.0, 128.7, 128.4, 127.0, 122.5, 121.6, 114.4, 113.0, 110.9, 60.8, 59.9, 36.2, 14.5, 14.5, 13.1	606.14
4e	2978, 1688, 1661, 1559, 1238, 816, 696	1.34–1.37 (m, 3H), 2.65–2.72 (m, 3H), 3.27–3.30 (m, 1H), 3.78–3.80 (m, 1H), 4.25–4.33 (m, 2H), 4.93–4.94 (m, 1H), 6.39–6.42 (m, 1H), 6.48 (s, 1H), 6.54 (s, 2H), 6.67–6.71 (m, 2H), 6.79–6.84 (m, 1H), 7.11–7.15 (m, 2H), 7.17.–7.19 (m, 1H), 7.21–7.23 (m, 1H), 7.26–7.29 (m, 1H), 7.33–7.37 (m, 2H), 10.70 (s, 1H)	173.2, 165.2, 148.6, 144.8, 144.6, 137.5, 136.8, 131.7, 131.6, 131.5, 131.5, 129.2, 128.7, 127.1, 122.6, 117.0, 116.2, 112.2, 110.4, 61.1, 59.8, 36.1, 14.5, 12.6	550.12
4f	3226, 1711, 1688, 1571, 1245, 823, 748, 697	1.33 (t, 3H), 2.70 (s, 3H), 3.26 (t, 1H), 3.69–3.72 (q, 1H, J = 2.93, J = 3.37) 4.22–4.31 (m, 2H), 4.90–4.93 (q, 1H, J = 3.53, J = 3.81), 6.50 (s, 1H), 6.51–6.62 (m, 2H), 6.76, 6.77 (d, 2H, J = 7.19), 6.82, 6.84 (d, 1H), 6.95–7.03 (m, 1H), 7.07–7.13 (m, 2H), 7.16–7.19 (m, 1H), 7.21–7.24 (m, 1H), 7.26–7.28 (m, 1H), 7.31–7.35 (m, 2H), 7.76, 7.77 (d, 1H, J = 7.19), 8.08 (s, 1H)	167.4, 165.4, 162.7, 140.9, 138.3, 136.4, 135.7, 134.2, 132.2, 131.7, 131.4, 130.5, 129.3, 129.1, 128.7, 127.1, 123.7, 122.6, 122.5, 119.8, 114.6, 110.9, 60.7, 59.8, 36.1, 14.5, 13.2	601.13

and were subsequently resuspended in phosphate buffer, pH 7.4. Test substances (25.0, 50.0 and 100.0 μmol L^{-1} in DMSO, final DMSO concentration < 0.1 %), positive (Triton X-100, 0.2 %) and negative (distilled water) controls were pipetted to 96-well plates and then erythrocyte suspension in phosphate buffer was added to each well. After incubation for 1 h at 37 °C, the plates were centrifuged at 500×*g* and the supernatant was transferred to new 96-well plates, and the absorbance of hemoglobin was measured at 430 nm in a Synergy 2 plate reader (BioTek Instruments). The results were represented as a percentage over positive controls' hemoglobin absorbance values, with the negative controls' values being accepted as zero hemolysis.

Radical scavenging activity determination. – 2,2-Diphenyl-1-picrylhydrazyl (DPPH) radical scavenging activity assay was performed to assess the antioxidant properties of compounds **3** and **4a**-**f** according to the method reported by Brand-Williams *et al*. (36). The samples were mixed with 0.56 mmol L^{-1} DPPH solution. The mixture was kept in dark for 30 min at 25 °C, after that the decrease in absorbance was measured at 517 nm. Trolox was used as a reference. All determinations were performed in triplicate.

In $ABTS^{\bullet+}$ assay the antioxidant activity of the obtained compounds **3**, **4a**-**f** was measured using a modification for 96-well plates in the method of Re *et al*. (37). The $ABTS^{\bullet+}$ radical solution was prepared by mixing ABTS (9.5 mL, 7 mmol L^{-1}) with potassium persulfate (245 μL, 100 mmol L^{-1}), reaching the final volume of 10 mL with distilled water. The solution was kept in dark for 18 h (at room temperature), and then diluted with potassium phosphate buffer (0.1 mol L^{-1}, pH 7.4) to an absorbance of 0.70 (± 0.02) at 734 nm. The samples were prepared in ethanol. The samples (50 μL) were placed in 96-well microplates and mixed thoroughly with 50 μL $ABTS^{\bullet+}$ radical working solution. Absorbance was measured at 734 nm. All determinations were performed in triplicate.

Isolation of rat liver microsomes and iron-ascorbic acid-induced lipid peroxidation assay (LPO). – The animals were fasted overnight and were sacrificed by cervical decapitation. Livers were thoroughly perfused with 1.15 % KCl and homogenized with four volumes of ice-cold 0.1 potassium phosphate buffer, pH = 7.4. The liver homogenate was centrifuged at 9 000×*g* for 30 min at 4 °C and the resulting postmitochondrial fraction (S9) was centrifuged at 105,000×*g* for 60 min at 4 °C. The microsomal pellets were re-suspended in 0.1 mol L^{-1} potassium phosphate buffer, pH = 7.4, containing 20 % glycerol. Microsomal protein content was determined according to Lowry *et al*. (38).

The microsomes were preincubated with compounds **3** and **4a-f** (20 μmol L^{-1}) at 37 °C for 30 min. The LPO was started with a solution of iron sulphate 20 μmol L^{-1} and ascorbic acid 0.5 mmol L^{-1} (39). The reaction was stopped after 20 min by adding a mixture of TCA 25 % and thiobarbituric acid (TBA) 0.67 %, and malondialdehyde (MDA) content was determined (40). The absorbance was measured at λ = 535 nm (Spectro UV-VIS Split spectrophotometer, Jenway, UK). The amount of MDA was calculated using a molar extinction coefficient of 1.56×10^5 L mol^{-1} cm^{-1}. The final results were presented as a percentage of only Fe^{2+}/AA-treated positive control (set as 100 %).

Statistical analysis

Statistically significant differences between IC_{50} values of each couple of compounds were detected based on the 95 % confidence intervals. The IC_{50} values and their respective confidence intervals were calculated by means of GraphPad Prism Software.

In some experiments, statistical analysis was performed by one-way ANOVA, followed by a Bonferroni test for multiple comparisons. Statistical evaluation was performed using the GraphPad Prism 5.0 software. Results are expressed as a mean ± SD ($n = 3$). Values of $p < 0.05$ were considered statistically significant.

RESULTS AND DISCUSSION

Syntheses and chemical characterization

The initial *N*-pyrrolylcarbohydrazide (**3**) was obtained through a multistage process, based on the classical Paal-Knorr cyclization for the synthesis of the initial *N*-pyrrolylcarboxylic acid (**1**), its esterification and as a final stage, selective hydrazinolysis of the obtained diester (**2**), as presented in Scheme 1. We observed that, while the hydrazinolysis of pyrrolecarboxylic esters was known to succeed at relatively severe conditions, hydrazinolysis of those non-conjugated with the pyrrole ring ester groups was found to be completed in a few hours in ethanol, due to the higher carbonyl activity (34). On the basis of this peculiarity, a selective hydrazinolysis was achieved with mixed-type diesters, which made possible the preservation of the ester groups in position-3 as a prerequisite for receptor binding (11, 34).

The general synthesis of the target hydrazones **4a-f** was carried out according to the procedures defined in Scheme 2, through condensation of the corresponding *N*-pyrrolylhydrazide (**3**) with any of the carbonyl compounds: 2-hydroxybenzaldehyde (**a**), 4-(dimethylamino)benzaldehyde (**b**), 4-methoxybenzaldehyde (**c**), 4-hydroxy-3-methoxybenzaldehyde (**d**) and furan-2-carbaldehyde (**e**) or indoline-2,3-dione (**f**) (Fig. 1).

The final hydrazones were synthesized in a micro synthesis apparatus, assuring about 62–93 % yields, low harmful emissions and reagent economy thus following the requirements of the green chemistry. The chemical names, melting points, yields and elemental analysis data for the obtained substances are presented in Table I.

The structures of the new compounds were elucidated with IR, ^{1}H and ^{13}C NMR spectral data and their purity was confirmed through elemental analysis. The spectral results corresponded with the assigned structures and are presented in Table II.

The IR spectra of the synthesized hydrazones **4a-f** revealed the presence of characteristic signals for two sets of amide I and amide II between 1680–1697 cm^{-1} and 1559–1571 cm^{-1}, resp. The observed bands in the range of 1709–1739 cm^{-1} pointed to the presence of the ester group at 3rd position in the pyrrole ring. The signals appearing between 3192 and 3226 cm^{-1} are characteristic for the presence of the hydrazide-hydrazone group.

In the obtained ^{1}H NMR spectra the NH signals for the CONH-N group were visible as a sharp singlet between 7.26 and 7.29 ppm. The characteristic signal for the C4 proton in the pyrrole ring is appearing as a singlet in the range of 6.37 to 6.50 ppm. In the spectral data are observed changes in the signals from the CH=N proton (a signal is missing in spectrum of **4f**), whereas the corresponding CH=N signals from the hydrazone group for all other derivatives are observed in the range from 7.81 to 10.70 ppm. The presence of the furan ring in the structure of **4e** shifts this signal to 7.72 ppm. Characteristic for the spectra are the triplet at 5.89 ppm and the doublet at 3.38 ppm for the phenyl fragment in the structure. In the obtained ^{13}C NMR spectra most characteristic is the signal for the CH=N group,

which is observed at 142.5 ppm for the substituted benzaldehyde fragments, while for the furan (**4e**) and isatin (**4f**) containing derivatives this signal is shifted to 152.9 and 134.8 ppm, resp. All NH and OH signals were D_2O exchangeable.

The chemical structures of the new compounds were supported by MS spectral data. Molecular ion peaks corresponding to the expected molecular masses were obtained for all compounds. The *m*/*z* values and the expected relative molecular masses are given in Table II, while the corresponding ^{1}H NMR and mass spectra are available as Supplementary Material.

Drug-likeness estimation with "Lipinski's rule of five"

The "Lipinski's rule of five" was applied for assessment of the reliability of the synthesized new *N*-pyrrolylhydrazide-hydrazones as possible prototypes for small molecules with favorable cell membrane permeability [including blood-brain barrier (BBB) permeability] and improved bioavailability.

According to the "Lipinski's rule of five", there are five key physicochemical parameters: molecular mass, lipophilicity, polar surface area, hydrogen bonding and charge, which have a significant impact on drug's BBB permeability, especially *via* passive diffusion. Poor BBB permeation is more likely to occur when there are more than 5 H-bond donors and 10 H-bond acceptors and when M_r is greater than 500 and calculated log*P* (Clog*P*) is greater than 5 (20). The effect of these physicochemical parameters on the interaction between the drug molecule and the lipophilic cell membrane is essential for the good pharmacokinetic behavior and lack of metabolism concerns for the new molecules designed as pharmacologically active substances (41).

The required Lipinski's parameters were calculated using the Molinspiration cheminformatics web server and the obtained results are presented in Table III.

Table III. Molecular parameters for the new compounds from Lipinski's rule of five

Compd.	Molecular parameter					%ABS
	log*P*	M_r	HBA	HBD	TPSA	
3	3.21	470.37	6	3	86.36	79.20
4a	6.57	574.48	7	2	92.93	76.93
4b	6.73	601.54	7	1	75.94	82.80
4c	6.68	588.50	7	1	81.94	80.73
4d	5.96	604.50	8	2	102.16	73.75
4e	5.88	548.44	7	1	85.84	79.38
4f	5.86	599.49	8	2	105.56	72.58

HBA – number of hydrogen bond acceptors, HBD – number of hydrogen bond donors,
TPSA – topological polar surface area

In addition, as a tool for oral absorption evaluation, the corresponding percentage absorption (%ABS) was also calculated for the target compounds, using the proposed formula (42):

$$\%ABS = 109 - 0.345 \times TPSA$$

where TPSA stands for topological polar surface area.

The obtained values for log*P* demonstrated that the target molecules possess hydrophobic properties which would facilitate their transport through the cell membranes and would contribute to a good absorption. The theoretical values for %ABS additionally confirm this observation. Except for the initial *N*-pyrrolylcarbohydrazide (**3**), all the target hydrazones violate the "Lipinski's rule of five" limitations for two parameters, log*P* and M_r with hydrophobic parameter log*P* being greater than 5 and molecular mass greater than 500, which should be considered and, if possible, avoided in future optimizations and design of other analogs.

Pharmacological evaluations

In vitro *cytotoxicity evaluation on HepG2 cells*. – The hepatotoxicity is one of the major causes of drug candidate withdrawals from the clinical studies and from the market (43, 44).

In order to check the safety profile of the newly synthesized compounds, we have evaluated their effect on the viability of HepG2 cells through the MTT (tetrazolium dye, 3-(4,5-dimethylthiazol-2-yl)-2,5-diphenyltetrazolium bromide) assay. HepG2 cells have proven to be an appropriate system for the preliminary evaluation of cytotoxicity for several chemical compounds (45, 46) including selected *N*-substituted pyrrolyl hydrazones, as they maintain many of the specialized functions of normal human hepatocytes (47, 48).

The calculated IC_{50} values of compounds **3** and **4a-f** are listed in Table IV. In general, all compounds (**3**, **4a**-**f**) did not show significant cytotoxicity against HepG2 cells. The corresponding IC_{50} values were in the range of 52.99–82.29 μmol L^{-1}. It should be noted that compounds **4a** and **4d**, with estimated IC_{50} values of 82.29 and 70.11 μmol L^{-1}, resp., were the least toxic, therefore, most perspective from a safety point of view, followed by **4f**, **4b**, **4e**, **3** and **4c**.

Hemolysis assay. – *In vitro* assessment of the hemolytic potential of the newly synthesized compounds is essential part of their toxicity evaluation. Therefore, we applied hemolysis test assay *in vitro* to determine the eventual interaction of the newly synthesized *N*-pyrrolylhydrazide hydrazones with blood components as a necessary part of their biocompatibility in early preclinical development. The effects of the test substances **3**, **4a-f** in isolated human erythrocytes were assayed as a function of a compound's concentration (25.0, 50.0 and 100.0 μmol L^{-1}) in erythrocyte suspensions as described in Experimental section. The hemolytic activity of the tested compounds was compared to the effects of Triton X 100 (0.2 %) in the same erythrocyte samples, as shown in Fig. 2. Triton induces complete hemolysis after 1 h of incubation (100 %). In contrast, all tested newly synthesized derivatives did not promote any hemolytic effects. In particular, we found that the hemolysis rate of the compounds **3** and **4a-f** at concentrations of up to 50 μmol L^{-1} was lower than 5 % and this result was up to the standard according to ISO/TR7405-1984(E). A slight

Table IV. IC_{50} *values for* in vitro *cytotoxicity evaluation of the target compounds*

Cmpd.	IC_{50} (μmol L^{-1})	95% confidence interval
3	54.88	56.62–56.17
4a	82.29	79.03–85.69
4b	58.39	55.48–61.46
4c	52.99	50.92–55.14
4d	70.11	65.59–74.93
4e	55.25	53.92–56.61
4f	63.31	61.96–64.69

[a] IC_{50} values for *in vitro* cytotoxicity evaluation of the target compounds as a robust parameter, appropriate for the comparison of overall cytotoxicity in a mechanism-independent manner.

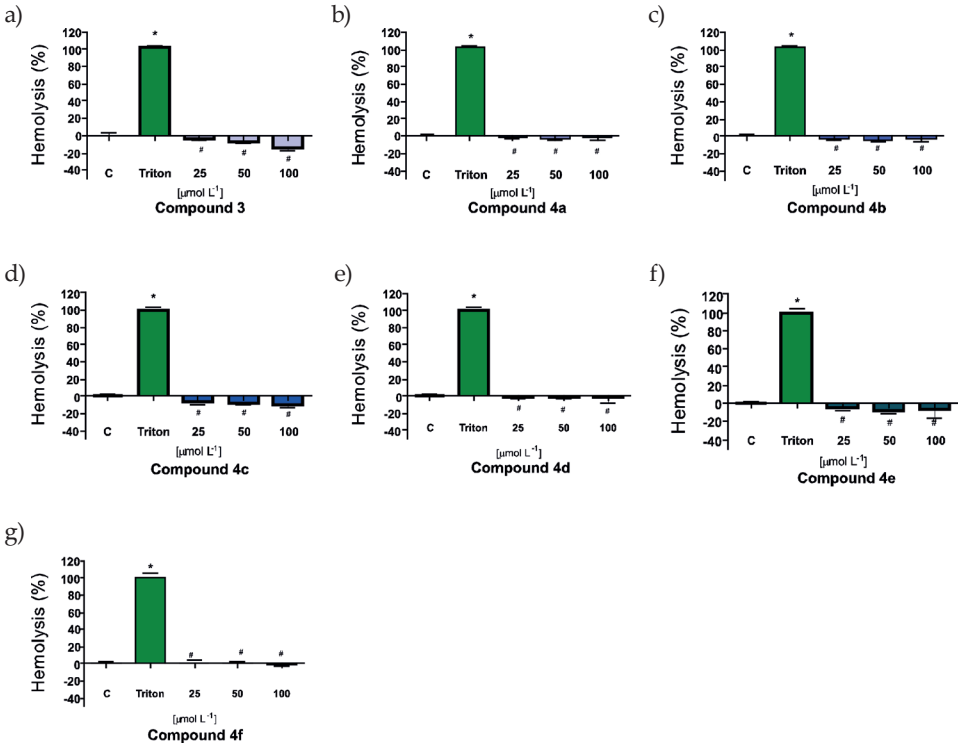

Fig. 2. Hemolytic effects of: a) compound **3** and b-g) compounds **4a-f** on human erythrocytes. The results are expressed as a mean ± SD of three independent experiments. Significant difference *vs.* control: *$p < 0.001$; *vs.* Triton X-100: #$p < 0.001$.

increase in hemolytic potential of **3**, **4c** and **4e** was observed at the concentration 100 μmol L^{-1}, but this concentration is quite high and unlikely to be used *in vivo*. Our results confirmed a good hemocompatibility of the tested hydrazones, indicating their appropriateness as potential pharmacophores. The safest and the most promising compounds were **4d** and **4a**, showing no hemolytic potential even at the highest tested concentration of 100 μmol L^{-1}.

DPPH assay. – The scavenging activity in DPPH (1,1-diphenyl-2-picrylhydrazyl) assay is attributed to the hydrogen donating ability of antioxidants. The antioxidant effects of compounds **3** and **4a-f** (31–250 μmol L^{-1}) were studied. The results are compared with those of Trolox at same concentrations and are presented in Fig. 3. At the applied concentrations Trolox is an effective scavenger of DPPH radical, in contrast to melatonin. Compounds **3** and **4d** scavenge DPPH radical in a concentration-dependent manner like Trolox, but less effectively than Trolox (Fig. 3).

The mechanism of antioxidant activity of compounds **4d** and **3** is most probably due to the reducing capacity, related to their chemical structure as pyrrole-based hydrazide-hydrazones. In fact, a recent study by Khan *et al.* (29) showed that 2,4,6-trichlorophenylhy-

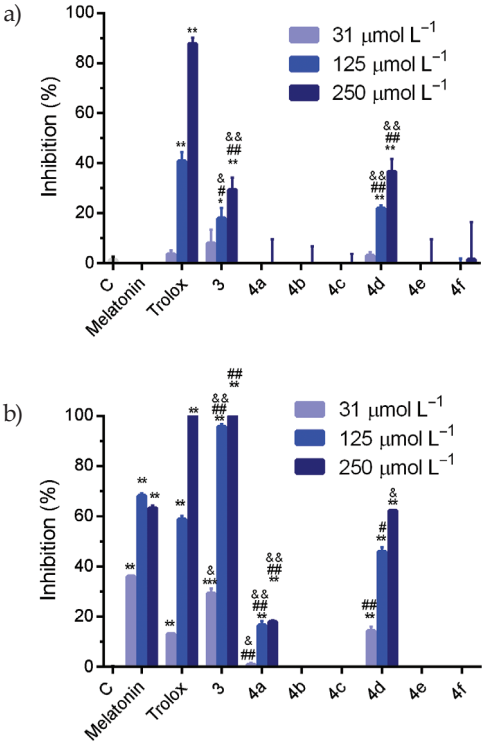

Fig. 3. Antioxidant capacity of compounds **3**, **4a-f**, applied at concentrations 31 to 250 μmol L^{-1}, determined by: a) DPPH and b) $ABTS^{*+}$ radical scavenging assays. Mean values of negative solvent controls (C) and experimental data ± standard deviation (SD) ($n = 3$). Significant difference *vs.* negative control: $^{*}p < 0.01$; $^{**}p < 0.001$; *vs.* melatonin: $^{\#}p < 0.01$, $^{\#\#}p < 0.001$; *vs.* Trolox: $^{\&}p < 0.01$, $^{\&\&}p < 0.001$.

drazine Schiff bases exhibited significant scavenging ability against DPPH radicals, the effect being attributed to their chemical structure. Sıcak *et al*. (49) also reported good antioxidant activity of novel fluorine-containing chiral hydrazide-hydrazones by means of their radical scavenging activity determined by ABTS and DPPH assays.

$ABTS^{\bullet+}$ radical decolorization assay. – In the applied concentrations (31–250 μmol L^{-1}), both Trolox and melatonin were effective antioxidants with melatonin being more effective at 31 μmol L^{-1} and Trolox at 250 μmol L^{-1}. Among the tested compounds, compound **3** is the most effective scavenger of $ABTS^{\bullet+}$ radical, being more effective than melatonin and Trolox. Compound **4d** showed favorable antioxidant activity at 250 μmol L^{-1} comparable to melatonin. Compound **4a** exerts a relatively week $ABTS^{\bullet+}$ radical scavenging activity while compounds **4b**, **4c**, **4e** and **4f** did not scavenge $ABTS^{\bullet+}$ radical at the applied concentrations (Fig. 3).

Fe^{2+}/AA-induced lipid peroxidation. – *In vitro* antioxidant properties of compounds **3**, **4a-f** were investigated in iron/ascorbic acid (Fe^{2+}/AA) induced lipid peroxidation in isolated rat liver microsomes (Fig. 4). This model system is commonly used for induction of non-enzymatic lipid peroxidation. None of the tested compounds (**3**, **4a-f**) induced lipid peroxidation in isolated rat liver microsomes as measured through malondialdehyde content, thus suggesting that they had no pro-oxidant activity itself (results not shown). In contrast, Fe^{2+}/AA treatment caused a significant (three-fold) increase in the amount of MDA *vs*. untreated controls. It was observed that Fe^{2+}/AA-induced lipid peroxidation was significantly attenuated in isolated rat liver microsomes by compounds **4d** and **3**, as measured by a decrease in MDA levels ($p < 0.001$). Melatonin (*N*-[2-(5-methoxy-1*H*-indol-3-yl)ethyl]-acetamide) was used as a reference substance, because of its well-known antioxidant and free radical scavenger properties (50–52). Melatonin decreased MDA levels by 37 % ($p < 0.001$). The protective effects of **4d** and **3** on lipid peroxidation were even higher than those of melatonin; they decreased MDA content by 82 and 58 %, resp. ($p < 0.001$) (Fig. 4). Compound **4f** dimin-

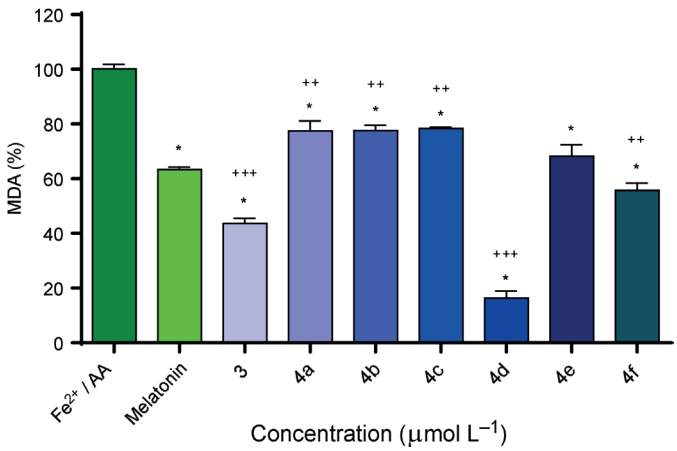

Fig. 4. Protective effects of compounds **3** and **4a-f** (20 μmol L^{-1}) on the levels of MDA in a model of Fe^{2+}/AA-induced lipid peroxidation in isolated rat liver microsomes. Data are normalized and presented as percentage of the Fe^{2+}/AA treated group (set as 100 %). Mean ± SD ($n = 3$). Significant difference *vs*. control (untreated microsomes): $^{*}p < 0.001$; *vs*. melatonin: $^{++}p < 0.01$, $^{+++}p < 0.001$.

ished the levels of MDA by 35 %, while the protective effects of compounds **4a**, **4b**, **4c** and **4e** were less pronounced, showing a decrease in MDA levels by 21, 22, 22 and 24 %, resp.

H_2O_2-induced oxidative stress in HepG2 cells. – Potential protective effects of compounds **3** and **4a-f** against oxidative stress induced by H_2O_2 in HepG2 cells were also investigated (Fig. 5). For this evaluation, we had selected the human hepatoma HepG2 cells as a well-

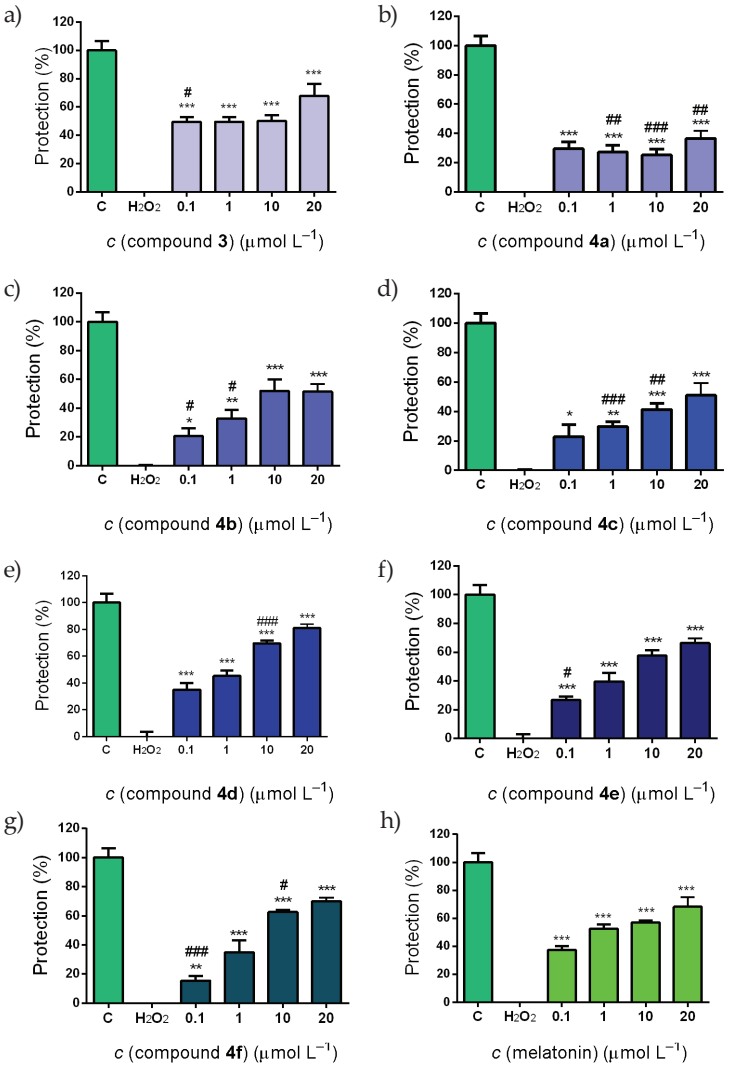

Fig. 5. Protective effects of the compounds **3** and **4a-f** on cell viability in H_2O_2-induced oxidative stress in HepG2 cells *in vitro*. Data are expressed as % protection; mean ± SD (n = 6). Significant difference *vs.* H_2O_2-treated controls: $^{*}p < 0.05$, $^{**}p < 0.01$, $^{***}p < 0.001$; *vs.* melatonin at respective concentration: $^{\#}p < 0.05$, $^{\#\#}p < 0.01$, $^{\#\#\#}p < 0.001$.

controlled, biological model system, characterized by stable phenotype, unlimited life span, high availability, expression of xenobiotic transcription factors, phase I and II drug metabolism enzymes and transporters (47). HepG2 cell line is an appropriate tool for studying the cytoprotective effects of different natural and synthetic compounds (53).

The cells were pre-treated with tested compounds at a concentration of 0.1, 1, 10 and 20 μmol L^{-1}, and then were exposed them to H_2O_2, as described in Experimental section. Cell mitochondrial function, measured by MTT-assay, was used as a marker to evaluate the effects on cell viability. The treatment with 0.1 mmol L^{-1} H_2O_2 (1 h) caused a significant decrease in cell viability by 42 % *vs.* untreated control cells ($p < 0.01$, results not shown). Pretreatment for 1 h of HepG2 cells with compound **4d** (0.1, 1, 10 and 20 μmol L^{-1}) significantly increased the cell survival by 35, 45, 69 and 81 %, resp., *vs.* H_2O_2 treatment (Fig. 5e). The antioxidant protection was even higher than that of the reference compound melatonin, which at the same concentrations increased the cell survival by 36, 52, 57 and 68 %, resp. (Fig. 5h). Significantly higher increase in survival compared to melatonin at 10 μmol L^{-1} was observed for **4a**, **4c**, **4d** and **4f** (Figs. 5b,d,e,g,h). Compounds **3** and **4e** were also effective, showing comparable effects to melatonin (Figs. 5a,f,h), whereas **4a**, **4b**, **4c** and **4f** showed lower antioxidant protection (Figs. 5b,c,d,g).

CONCLUSIONS

One new *N*-pyrrolylcarbohydrazide (**3**) and six new *N*-pyrrole hydrazones (**4a-f**) were synthesized. Except for the initial *N*-pyrrolylcarbohydrazide, all target hydrazones violate the "Lipinski's rule of five" limitations on two parameters, log*P* and M_r. On the other hand, all compounds possess hydrophobic properties which would facilitate their passing through the cell membranes and would contribute to a good absorption. This conclusion is further confirmed by the high values of %ABS. The *in vitro* safety screening tests for cytotoxicity on HepG2 cells and hemocompatibility (hemolysis assay) showed good safety profile of the new compounds with **4d** and **4a** defined as the least toxic. The *in vitro* antioxidant activities of the newly-synthesized compounds **3** and **4a-f** was assessed by DPPH and $ABTS^{*+}$ tests and showed that compound **3** was the most potent radical scavenger, followed by **4d** in $ABTS^{\bullet+}$ radical discoloration assay, whereas **4d** was slightly better in DPPH assay. Further, our *in vitro* protection study proved efficient prevention against oxidative stress in H_2O_2-induced injury in HepG2 cells, especially by compounds **4d** and **3**. Both compounds (**4d** and **3**) were also the most effective protectors in the model of Fe^{2+}/AA-induced lipid peroxidation, showing a significant attenuation of peroxidation in isolated rat liver microsomes. This study revealed that the most promising compounds with potent antioxidant activity were **4d** and **3**. Nevertheless, **4d** possesses a better safety profile than all other evaluated newly-synthesized compounds and was proven as the most perspective for further investigations of pharmacological properties.

REFERENCES

1. G. Lavanya, V. Padmavathi and A. Padmaja, Synthesis and antioxidant activity of 1,4-[bis(3-arylmethanesulfonyl pyrrolyl and pyrazolyl)]benzenes, *J. Braz. Chem. Soc.* **25** (2014) 1200–1207; https://doi.org/10.5935/0103-5053.20140097

2. S. Durgamma, A. Muralikrishna, V. Padmavathi and A. Padmaja, Synthesis and antioxidant activity of amido-linked benzoxazolyl/benzothiazolyl/benzimidazolyl-pyrroles and pyrazoles, *Med. Chem. Res.* **23** (2014) 2916–2929; https://doi.org/10.1007/s00044-013-0884-x
3. S. K. Sridhar, M. Saravanan and A. Ramesh, Synthesis and antibacterial screening of hydrazones, Schiff and Mannich bases of isatin derivatives, *Eur. J. Med. Chem.* **36** (2001) 615–625; https://doi.org/10.1016/S0223-5234(01)01255-7
4. S. I. Alqasoumi, M. M. Ghorab, Z. H. Ismail, S. M. Abdel-Gawad, M. S. El-Gaby and H. M. Aly, Novel antitumor acetamide, pyrrole, pyrrolopyrimidine, thiocyanate, hydrazone, pyrazole, isothiocyanate and thiophene derivatives containing a biologically active pyrazole moiety, *Arzneimittelforschung* **59** (2009) 666–671; https://doi.org/10.1055/s-0031-1296457
5. Y. Xia, C. Fan, B. X. Zhao, J. Zhao, D. S. Shin and J. Y. Miao, Synthesis and structure-activity relationships of novel 1-arylmethyl-3-aryl-1*H*-pyrazole-5-carbohydrazide hydrazone derivatives as potential agents against A549 lung cancer cells, *Eur. J. Med. Chem.* **43** (2008) 2347–2353; https://doi.org/10.1016/j.ejmech.2008.01.021
6. R. M. Mohareb, H. D. Fleita and O. K. Sakka, Novel synthesis of hydrazide-hydrazone derivatives and their utilization in the synthesis of coumarin, pyridine, thiazole and thiophene derivatives with antitumor activity, *Molecules* **16** (2010) 16–27; https://doi.org/10.3390/molecules16010016
7. A. A. El-Tombary and S. A. M. El-Hawash, Synthesis, antioxidant, anticancer and antiviral activities of novel quinoxalinehydrazone derivatives and their acyclic C-nucleosides, *Med. Chem.* **10** (2014) 521–532; https://doi.org/10.2174/1573406411309666006 9
8. M. O. Puskullu, H. Shirinzadeh, M. Nenni, H. Gurer-Orhan and S. Suzen, Synthesis and evaluation of antioxidant activity of new quinoline-2-carbaldehyde hydrazone derivatives: bioisosteric melatonin analogues, *J. Enzyme Inhib. Med. Chem.* **31** (2016) 121–125; https://doi.org/10.3109/14756366.2015.1005012
9. H. S. Kareem, A. Ariffin, N. Nordin, T. Heidelberg, A. Abdul-Aziz, K. W. Kong and W. Yehye, Correlation of antioxidant activities with theoretical studies for new hydrazone compounds bearing a 3,4,5-trimethoxy benzyl moiety, *Eur. J. Med. Chem.* **103** (2015) 497–505; https://doi.org/10.1016/j.ejmech.2015.09.016
10. M. Georgieva, D. Tzankova, S. Vladimirova and A. Bijev, Evaluation of a group of pyrrole derivatives as tuberculostatic agents, *CBU Int. Conf. Innov. Sci. Ed.* **5** (2017) 1083–1091; https://doi.org/10.12955/cbup.v5.1075
11. A. Bijev and M. Georgieva, Pyrrole-based hydrazones synthesized and evaluated in vitro as potential tuberculostatics, *Lett. Drug Des. Discov.* **7** (2010) 430–437; https://doi.org/10.2174/157018009789108268
12. A. Kajal, S. Bala, N. Sharma, S. Kamboj and V. Saini, Therapeutic potential of hydrazones as anti-inflammatory agents, *Int. J. Med. Chem.* **11** (2014) 1–11; https://doi.org/10.1155/2014/761030
13. K. N. de Oliveira, P. Costa, J. R. Santin, L. Mazzambani, C. Bürger, C. Mora, R. J. Nunes and M. M. de Souza, Synthesis and antidepressant-like activity evaluation of sulphonamides and sulphonylhydrazones, *Bioorg. Med. Chem.* **19** (2011) 4295–4306; https://doi.org/10.1016/j.bmc.2011.05.056
14. C. M. Leal, S. L. Pereira, A. E. Kummerle, D. M. Leal, R. Tesch, C. M. de Sant'Anna, C. A. Fraga, E. J. Barreiro, R. T. Sudo and G. Zapata-Sudo, Antihypertensive profile of 2-thienyl-3,4-methylene dioxy benzoylhydrazone is mediated by activation of the A2A adenosine receptor, *Eur. J. Med. Chem.* **55** (2012) 49–57; https://doi.org/10.1016/j.ejmech.2012.06.056
15. L. Yurttaş, Y. Özkay, Z. A. Kaplancıklı, Y. Tunalı and H. Karaca, Synthesis and antimicrobial activity of some new hydrazone-bridged thiazole-pyrrole derivatives, *J. Enzyme Inhib. Med. Chem.* **28** (2013) 830–835; https://doi.org/10.3109/14756366.2012.688043
16. O. O. Ajani, C. A. Obafemi, O. C. Nwinyi and D. A. Akinpelu, Microwave assisted synthesis and antimicrobial activity of 2-quinoxalinone-3-hydrazone derivatives, *Bioorg. Med. Chem.* **18** (2010) 214–221; https://doi.org/10.1016/j.bmc.2009.10.064

17. R. J. Vaigunda, D. Sriram, S. K. Patel, I. V. Reddy, N. Bharathwajan, J. Stables and P. Yogeeswari, Design and synthesis of anticonvulsants from a combined phthalimide-GABA-anilide and hydrazone pharmacophore, *Eur. J. Med. Chem.* **42** (2007) 146–151; https://doi.org/10.1016/j.ejmech.2006.08.010
18. J. R. Dimmock, S. C. Vashishtha and J. P. Stables, Anticonvulsant properties of various acetylhydrazones, oxamoylhydrazones and semicarbazones derived from aromatic and unsaturated carbonyl compounds, *Eur. J. Med. Chem.* **35** (2000) 241–248; https://doi.org/10.1016/S0223-5234(00)00123-9
19. B. G. Giménez, M. S. Santos, M. Ferrarini and J. P. S. Fernandes, Evaluation of blockbuster drugs under the Rule-of-five, *Pharmazie* **65** (2010) 148–152; https://doi.org/10.1691/ph.2010.9733
20. C. A. Lipinski, Lead- and drug-like compounds: the rule-of-five revolution, *Drug Discov. Today Technol.* **1** (2004) 337–341; https://doi.org/10.1016/j.ddtec.2004.11.007
21. T. P. Kenakin, *Pharmacology in Drug Discovery and Development*, 2nd ed., Elsevier, Amsterdam 2017, pp. 157–191.
22. J. F. Varghese, R. Patel and U. C. S. Yadav, Novel insights in the metabolic syndrome-induced oxidative stress and inflammation-mediated atherosclerosis, *Curr. Cardiol. Rev.* **14** (2018) 4–14; https://doi.org/10.2174/1573403X13666171009112250
23. H. Yaribeygi, Y. Panahi, B. Javadi and A. Sahebkar, The underlying role of oxidative stress in neurodegeneration: A mechanistic review, *CNS Neurol. Dis.-Drug Targets* **17** (2018) 207–215; https://doi.org/10.2174/1871527317666180425122557
24. L. A. Pham-Huy, H. He and C. Pham-Huy, Free radicals, antioxidants in disease and health, *Int. J. Biomed. Sci.* **4** (2008) 89–96.
25. M. Chand, Rajeshwari, A. Hiremathad, M. Singh, M. A. Santos and R. S. Keri, A review on antioxidant potential of bioactive heterocycle benzofuran: Natural and synthetic derivatives, *Pharmacol. Rep.* **69** (2017) 281–295; https://doi.org/10.1016/j.pharep.2016.11.007
26. M. Miceli, E. Roma, P. Rosa, M. Feroci, M. A. Loreto, D. Tofani and T. Gasperi, Synthesis of benzofuran-2-one derivatives and evaluation of their antioxidant capacity by comparing DPPH assay and cyclic voltammetry, *Molecules* **23** (2018) 710–726; https://doi.org/10.3390/molecules23040710
27. A. A. Shanty, J. E. Philip, E. J. Sneha, M. R. P. Kurup, S. Balachandran and P. V. Mohanan, Synthesis, characterization and biological studies of Schiff bases derived from heterocyclic moiety, *Bioorg. Chem.* **70** (2017) 67–73; https://doi.org/10.1016/j.bioorg.2016.11.009
28. A. A. Shanty and P. V. Mohanan, Heterocyclic Schiff bases as non toxic antioxidants: Solvent effect, structure activity relationship and mechanism of action, *Spectrochim. Acta A* **192** (2018) 181–187; https://doi.org/10.1016/j.saa.2017.11.019
29. K. M. Khan, Z. Shah, V. U. Ahmad, M. Khan, M. Taha, F. Rahim, S. Ali, N. Ambreen, S. Perveen, M. I. Choudhary and W. Voelter, 2,4,6-Trichlorophenylhydrazine Schiff bases as DPPH radical and superoxide anion scavengers, *Med. Chem.* **8** (2012) 452–461; https://doi.org/10.2174/1573406411208030452
30. N. Belkheiri, B. Bouguerne, F. Bedos-Belval, H. Duran, C. Bernis, R. Salvayre, A. Nègre-Salvayre and M. Baltas, Synthesis and antioxidant activity evaluation of a syringic hydrazones family, *Eur. J. Med. Chem.* **45** (2010) 3019–3026; https://doi.org/10.1016/j.ejmech.2010.03.031
31. A. Guillouzo, Liver cell models in in vitro toxicology, *Environ. Health Perspect.* **106** (Suppl. 2) (1998) 511–532; https://doi.org/10.1289/ehp.98106511
32. P. Ertl, B. Rohde and P. Selzer, Fast calculation of molecular polar surface area as a sum of fragment-based contributions and its application to the prediction of drug transport properties, *J. Med. Chem.* **43** (2000) 3714–3717; https://doi.org/10.1021/jm000942e
33. D. F. Veber, S. R. Johnson, H. Y. Cheng, B. R. Smith, K. W. Ward and K. D. Kopple, Molecular properties that influence the oral bioavailability of drug candidates, *J. Med. Chem.* **45** (2002) 2615–2623; https://doi.org/10.1021/jm020017n

34. A. Bijev, Synthesis and preliminary screening of carbohydrazides and hydrazones of pyrrole derivatives as potential tuberculostatics, *Arzneimittelforschung* **56** (2006) 96–103; https://doi.org/10.1055/s-0031-1296708

35. B. C. Evans, C. E. Nelson, S. S. Yu, K. R. Beavers, A. J. Kim, H. Li, H. M. Nelson, T. D. Giorgio and C. L. Duvall, Ex vivo red blood cell hemolysis assay for the evaluation of pH-responsive endosomolytic agents for cytosolic delivery of biomacromolecular drugs, *J. Vis. Exp.* **73** (2013) e50166; https://doi.org/10.3791/50166

36. W. Brand-Williams, M. E. Cuvelier and C. Berset, Use of a free radical method to evaluate antioxidant activity, *LWT-Food Sci. Technol.* **28** (1995) 25–30; https://doi.org/10.1016/S0023-6438(95)80008-5

37. R. Re, N. Pellegrini, A. Proteggente, A. Pannala, M. Yang and C. Rice-Evans, Antioxidant activity applying an improved ABTS radical cation decolorization assay, *Free Radic. Biol. Med.* **26** (1999) 1231–1237; https://doi.org/10.1016/S0891-5849(98)00315-3

38. O. H. Lowry, N. J. Rosebrough, A. L. Farr and R. J. Randall, Protein measurement with the Folin phenol reagent, *J. Biol. Chem*. **193** (1951) 265–275.

39. D. Mansuy, A. Sassi, P. M. Dansette and M. Plat, A new potent inhibitor of lipid peroxidation *in vitro* and *in vivo*, the hepatoprotective drug anisyldithiolthione, *Biochem. Biophys. Res. Commun*. **135** (1986) 1015–1021; https://doi.org/10.1016/0006-291X(86)91029-6

40. C. Deby and R. Goutier, New perspectives on the biochemistry of superoxide anion and the efficiency of superoxide dismutases, *Biochem. Pharmacol*. **39** (1990) 399–405; https://doi.org/10.1016/0006-2952(90)90043-K

41. H. Gao and X. Gao, *Recent Progress in Blood-brain Barrier Transportation Research,* in *Brain Targeted Drug Delivery System – A Focus on Nanotechnology and Nanoparticulates,* 1st ed. Elsevier, Amsterdam 2019, pp. 469–481.

42. Y. H. Zhao, M. H. Abraham, J. Lee, A. Hersey, C. N. Luscombe, G. Beck, B. Sherborne and I. Cooper, Rate-limited steps of human oral absorption and QSAR studies, *Pharm. Res.* **19** (2002) 1446–1457.

43. D. Schuster, C. Laggner and T. Langer, Why drugs fail – a study on side effects in new chemical entities, *Curr. Pharm. Des.* **11** (2005) 3545–3559; https://doi.org/10.2174/138161205774414510

44. W. C. Maddrey, Drug-induced hepatotoxicity, *J. Clin. Gastroenterol*. **39** (2005) S83–S89; https://doi.org/10.1097/01.mcg.0000155548.91524.6e

45. J. Hou, W. Zhao, Z. N. Huang, S. M. Yang, L. J. Wang, Y. Jiang, Z. S. Zhou, M. Y. Zheng, J. L. Jiang, S. H. Li and F. N. Li, Evaluation of novel *N*-(piperidine-4-yl)benzamide derivatives as potential cell cycle inhibitors in HepG2 cells, *Chem. Biol. Drug Des.* **86** (2015) 223–231; https://doi.org/10.1111/cbdd.12484

46. P. Martins, J. Jesus, S. Santos, L. R. Raposo, C. Roma-Rodrigues, P. V. Baptista and A. R. Fernandes, Heterocyclic anticancer compounds: recent advances and the paradigm shift towards the use of nanomedicine's tool box, *Molecules* **20** (2015) 16852–16891; https://doi.org/10.3390/molecules200916852

47. S. Knasmüller, W. Parzefall, R. Sanyal, S. Ecker, C. Schwab, M. Uhl, V. Mersch-Sundermann, G. Williamson, G. Hietsch, T. Langer, F. Darroudi and A. T. Natarajan, Use of metabolically competent human hepatoma cells for the detection of mutagens and antimutagens, *Mutat. Res./Fund. Mol. Mech. Mutagen.* **402** (1998) 185–202; https://doi.org/10.1016/S0027-5107(97)00297-2

48. V. Mersch-Sundermann, S. Knasmüller, X. J. Wu, F. Darroudi and F. Kassie, Use of a human-derived liver cell line for the detection of cytoprotective, antigenotoxic and cogenotoxic agents, *Toxicology* **198** (2004) 329–340; https://doi.org/10.1016/j.tox.2004.02.009

49. Y. Sıcak, E. E. Oruç-Emre, M. Öztürk, T. Taşkın-Tok and A. Karaküçük-Iyidoğan, Novel fluorine-containing chiral hydrazide-hydrazones: Design, synthesis, structural elucidation, antioxidant and anticholinesterase activity, and *in silico* studies, *Chirality* (2019) https://doi.org/10.1002/chir.23102; ahead of print.

50. D. X. Tan, L. D. Chen, B. Poeggeler, L. C. Manchester and R. J. Reiter, Melatonin: a potent, endogenous hydroxyl radical scavenger, *Endocr. J.* **1** (1993) 57–60.
51. R. Reiter, L. Tang, J. J. Garcia and A. Munoz-Hoyos, Pharmacological actions of melatonin in oxygen radical pathophysiology, *Life Sci.* **60** (1997) 2255–2271; https://doi.org/10.1016/S0024-3205(97)00030-1
52. R. Hardeland, Antioxidative protection by melatonin: multiplicity of mechanisms from radical detoxification to radical avoidance, *Endocrine* **27** (2005) 119–130; https://doi.org/10.1385/ENDO:27:2:119
53. L. Deferme, J. J. Briedé, S. M. H. Claessen, D. G. J. Jennen, R. Cavill and J. C. S. Kleinjans, Time series analysis of oxidative stress response patterns in HepG2: a toxicogenomics approach, *Toxicology* **306** (2013) 24–34; https://doi.org/10.1016/j.tox.2013.02.001